Electronic Supplementary Material (ESI) for Journal of Materials Chemistry A.

Supporting Information

A low cost Zn^{2+}/I^- redox active electrolyte for a high energy and long cycle-life zinc hybrid battery-capacitor

Balamurugan Selvaraj, Balaji Sambandam, Sungjin Kim, Vinod Mathew, Sehong Seo, Moonsu Song and Jaekook Kim*

Department of Materials Science and Engineering, Chonnam National University, 300 Yongbong-dong, Bukgu, Gwangju, 500-757, South Korea.

*Corresponding author: E-mail: jaekook@chonnam.ac.kr; Fax: +82-62-530-1699; Tel: +82-62-530-1703

Experimental

Materials

Gelatin, potassium hydroxide (KOH), potassium iodide (KI), zinc iodide (ZnI_2), zinc sulfate monohydrate ($ZnSO_4.H_2O$), N-methyl-2-pyrrolidone (NMP), and poly acrylic acid (PAA) were purchased from Sigma Aldrich chemicals and used without any purification.

Synthesis of porous carbon

The precursor gelatin was heated at 650 °C in a highly equipped quartz tubular furnace under Argon atmosphere and maintained for 1 h to complete the carbonization process. Subsequently, the obtained carbon and activation agent KOH were mixed in 1:3 weight ratio, heated up to 750 °C at an increasing rate of 10 °C/min and the activation was maintained for 1 h under Ar condition. After activation, the dark black powder was washed thoroughly with HCl and distilled water to eliminate the residual alkali completely and dried in a hot air oven at 100°C for 12 h to obtain the final activated porous carbon (PC) product.

Instrumentation

Powder X-ray diffraction (PXRD) for synthesized porous carbon material was analyzed using a Shimadzu X-ray diffractometer (Cu Kα radiation, k = 1.5406 Å). The porous morphology of the prepared PC was determined by the instruments, S-4700 Hitachi (field emission scanning electron microscopy, FE-SEM) and Philips Tecnai F20 at 200 kV (field emission transmission electron microscopy, FE-TEM), KBSI, Chonnam National University, respectively. Elemental analysis was conducted on a EDX analyzer (EMAX Energy EX-200, Horiba) attached to a F20 microscope. The specific surface area and pore parameters were acquired by N_2 adsorption/desorption studies using a Micromeritics ASAP2010 instrument based on the Brunauer–Emmett–Teller (BET,) method. The graphitization degree of PC was detected by Raman spectra using a JASCO Raman spectrometer, NRS-5100 with a 532 nm laser line. The elemental oxidation states in PC were obtained by X-ray photoelectron spectroscopy (XPS, Thermo VG Scientific instrument, Multilab 2000) with Al Kα as the X-ray source.

An active material (PC), conducting carbon (super P), and binder poly acrylic acid (PAA) in the weight ratio of 80:10:10 in NMP were mixed as a viscous slurry to act as the cathode. The cathode slurry was then uniformly coated on a stainless-steel foil (current

collector) by doctor blade method and dried overnight in a vacuum oven at 100 °C. It was then hot pressed over stainless-steel rollers at 100 °C and punched into circular discs. The loaded active material was found to be 2.7-3.2 mg/cm^2. A 2032-type coin cell was made-up by a cathode, a separator (Glass fiber) and anode (zinc foil). An aqueous solution of 1 M $ZnSO_4$, 2 M $ZnSO_4$, 1 M $ZnSO_4$ + 0.04 M KI, 2 M $ZnSO_4$ + 0.04 M KI, 1 M $ZnSO_4$ + 0.08 M KI, 2 M $ZnSO_4$ + 0.08 M KI, 1 M $ZnSO_4$ + 0.16 M KI, 2 M $ZnSO_4$ + 0.16 M KI and 1 M $ZnSO_4$ + 0.08 M ZnI_2 were used as electrolytes respectively. The pH of the electrolytes employed varied from ~ 4.96 to 5.45 (**Fig. S1**). The price of the KI and ZnI_2 additives are given in the **Table S2**. Electrochemical analysis of the assembled cells was examined using a multi-channel BTS 2004H battery tester (Nagano Keiki Co. Ltd., Tokyo, Japan) in the 0.2-1.8 (vs. Zn/Zn^{2+}) voltage range. Moreover, cyclic voltammetry (CV) and Electrochemical impedance spectrum (EIS) experiments were conducted in a Biologic VSP potentiostat instrument.

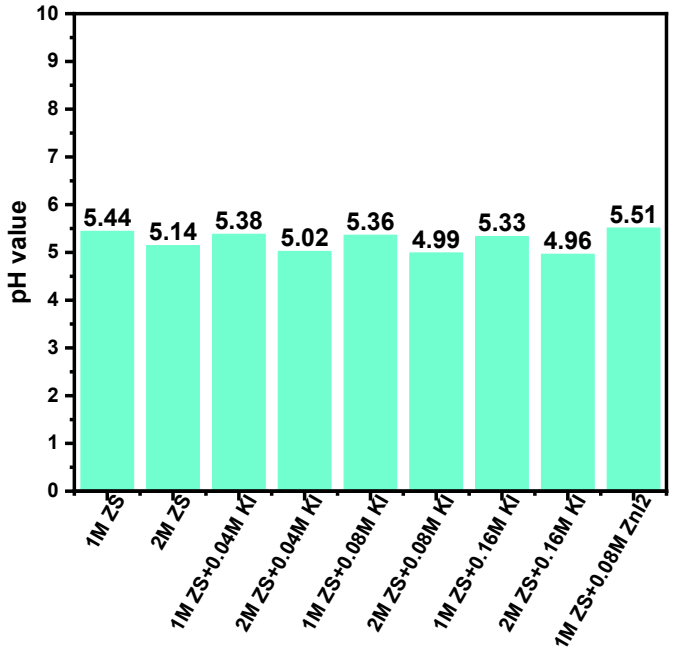

Fig. S1 pH values of the aqueous zinc electrolytes.

Table S1 Elemental analysis of PC.

Sample Name	Nitrogen	Carbon	Hydrogen
PC	1.112	54.515	4.484

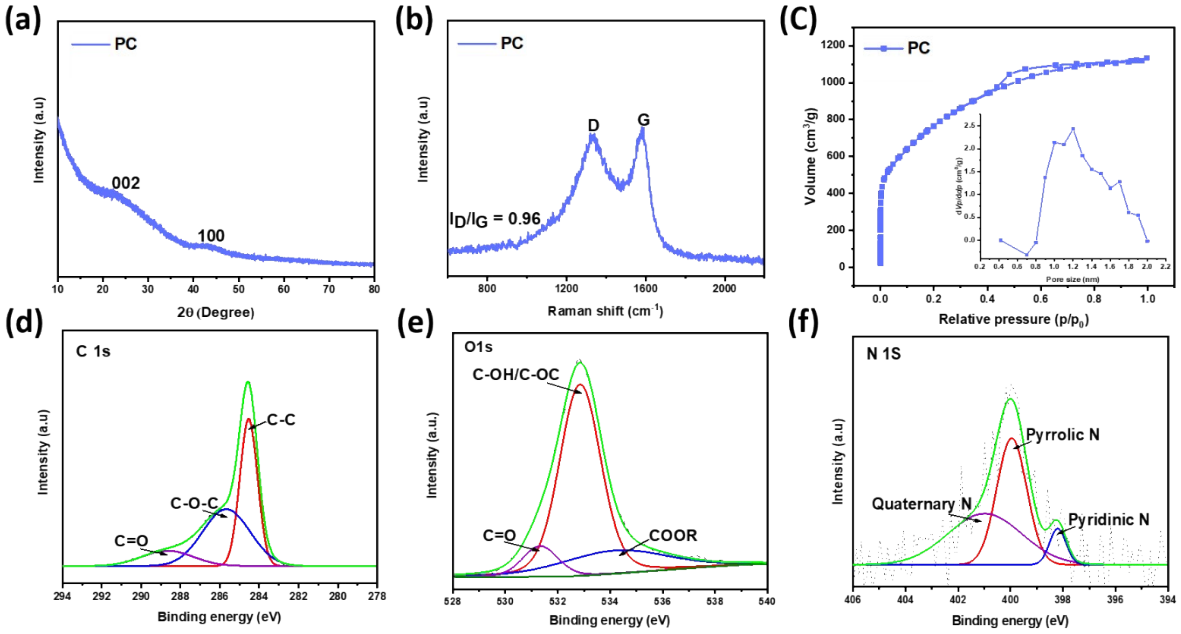

Fig. S2 (a) XRD pattern, (b) Raman spectrum, (c) Nitrogen adsorption–desorption isotherms with pore-size distribution plot (inset), (d) XPS C1s, (e) XPS O1s, and (f) XPS N1s spectra of PC cathode.

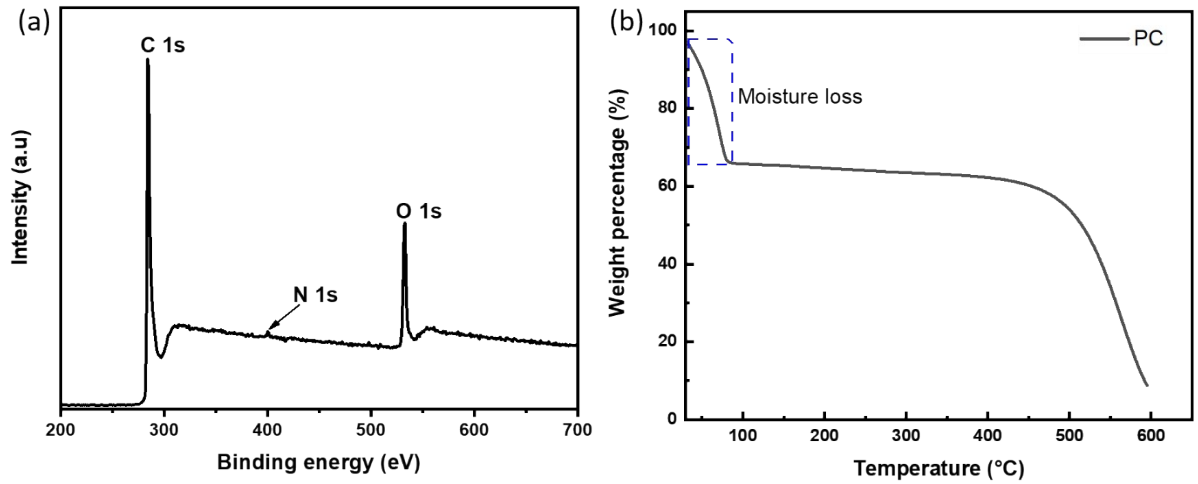

Fig. S3 (a) XPS survey spectrum and (b) TGA of PC.

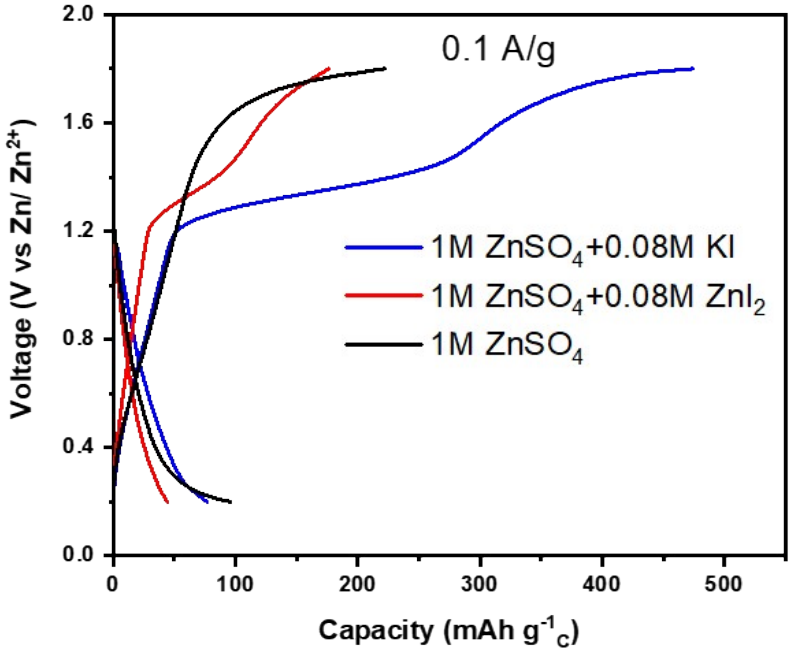

Fig. S4 Comparative initial discharge/charge curves of fabricated ZHC cell with electrolytes 1M $ZnSO_4$, and AZHBC cells with electrolytes 1M $ZnSO_4$ + 0.08 M ZnI_2, and 1M $ZnSO_4$ + 0.08 M KI at a current density of 0.1 A g^{-1}.

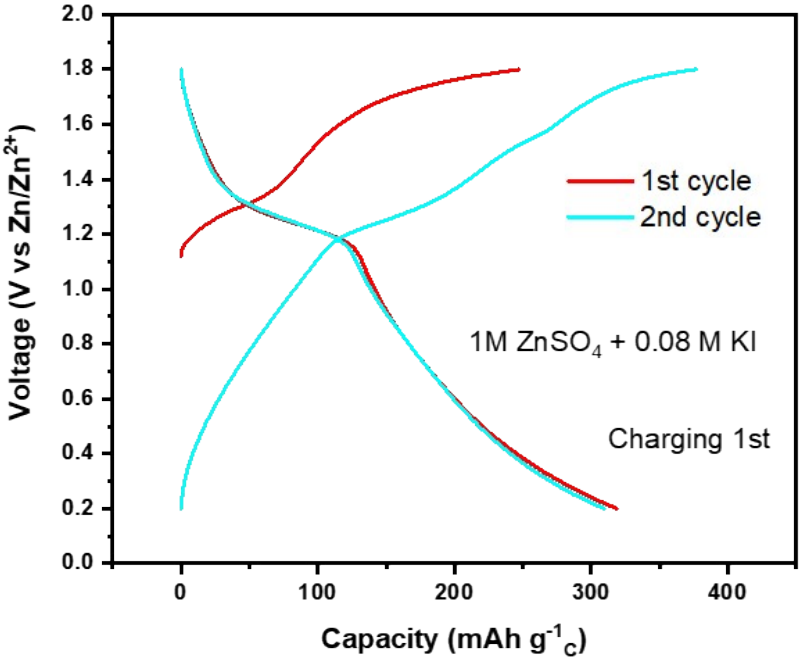

Fig. S5 Initial charge/discharge curves of fabricated AZHBC cells with electrolytes 1M $ZnSO_4$ + 0.08 M KI at a current density of 0.1 A g^{-1}.

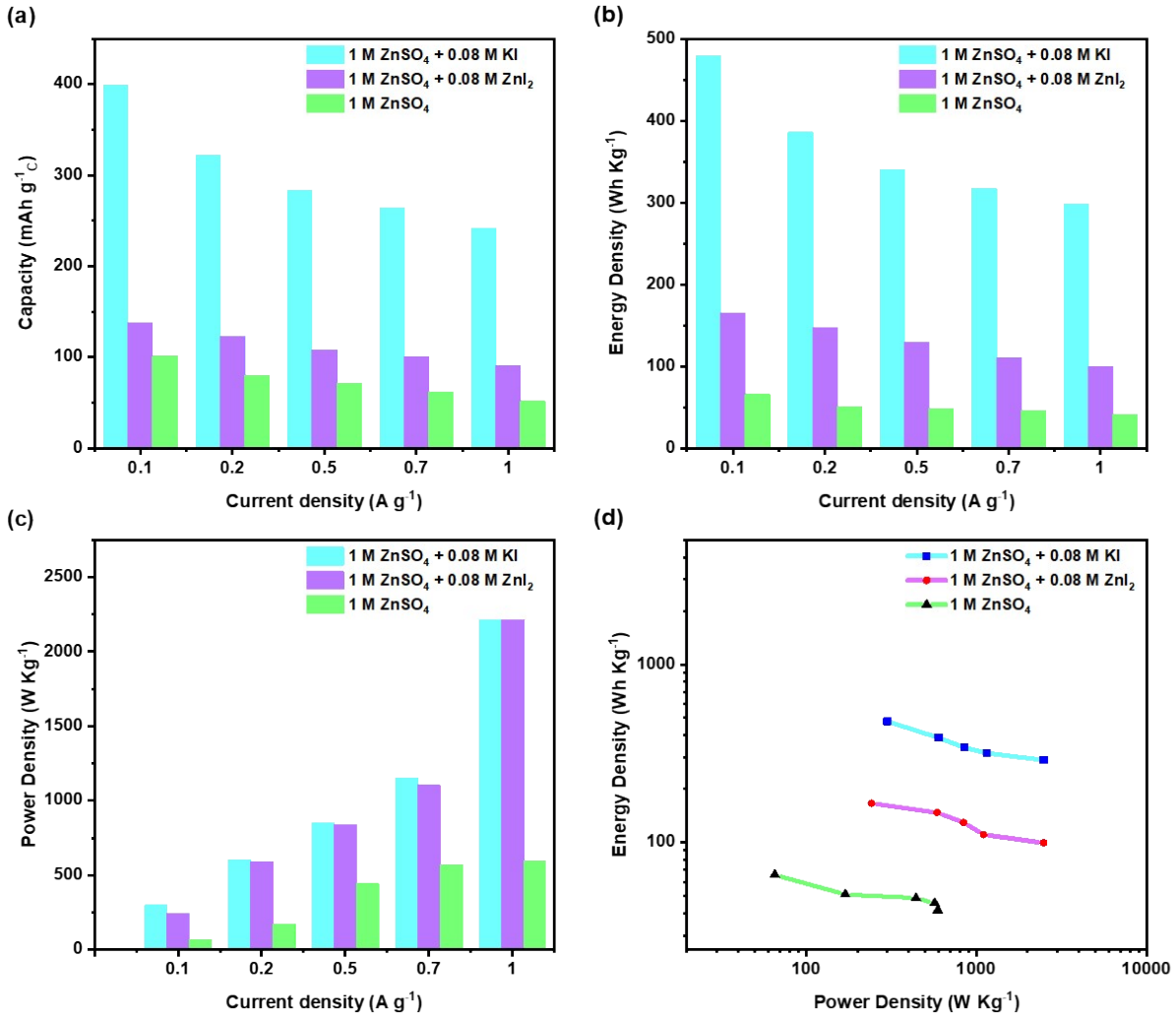

Fig. S6 (a) Specific capacities, (b) Energy densities, (c) Power densities at current densities from 0.1 to 1 A g^{-1} and (d) Rangone plots of ZHC cells with electrolyte 1M $ZnSO_4$, and AZHBC cells with electrolytes 1M $ZnSO_4$ + 0.08 M ZnI_2, and 1M $ZnSO_4$ + 0.08 M KI respectively.

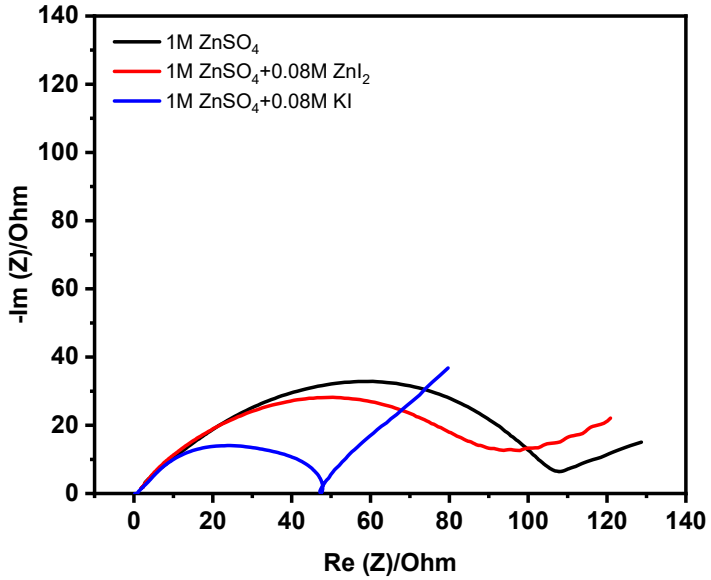

Fig. S7 Comparative EIS curves of fabricated ZHC cells with electrolytes 1M $ZnSO_4$, and AZHBC cells with electrolytes 1M $ZnSO_4$ + 0.08 M ZnI_2, and 1M $ZnSO_4$ + 0.08 M KI.

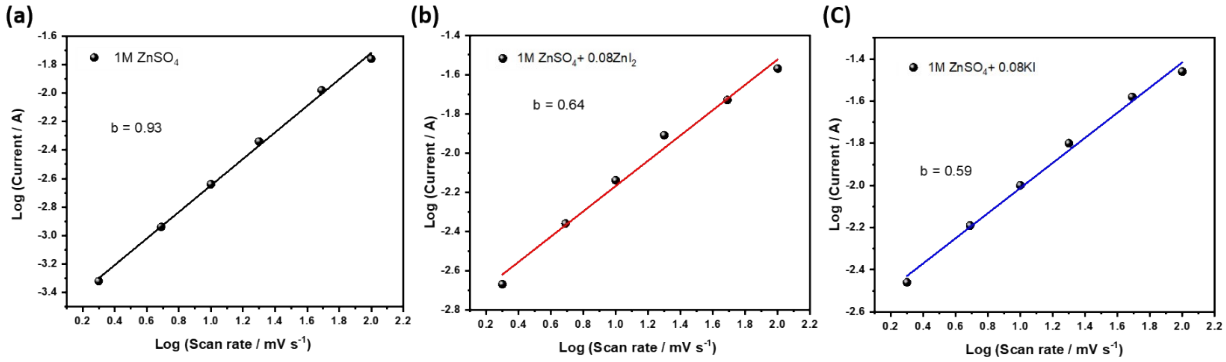

Fig. S8 Linear fit of log(v) and log(i) of fabricated ZHC cells with electrolytes (a) 1M $ZnSO_4$, and AZHBC cells with electrolytes (b) 1M $ZnSO_4$ + 0.08 M ZnI_2, and (c) 1M $ZnSO_4$ + 0.08 M KI.

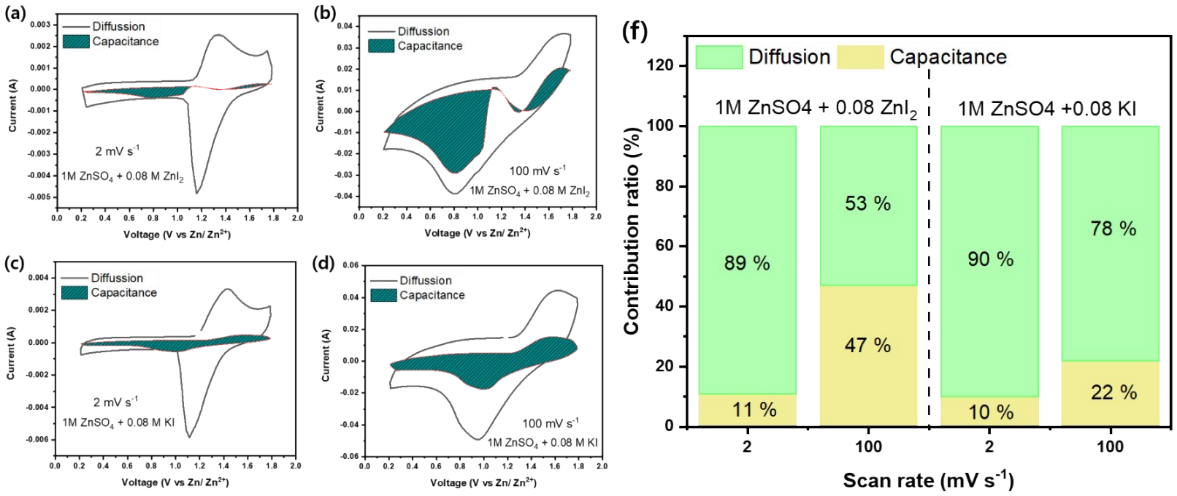

Fig. S9 Diffusion and capacitance contribution plots of AZHBC cells with electrolytes (a & b) 1M $ZnSO_4$ + 0.08 M ZnI_2, (c & d) 1M $ZnSO_4$ + 0.08 M KI and (f) bar diagram of contribution ratios at different scan rates.

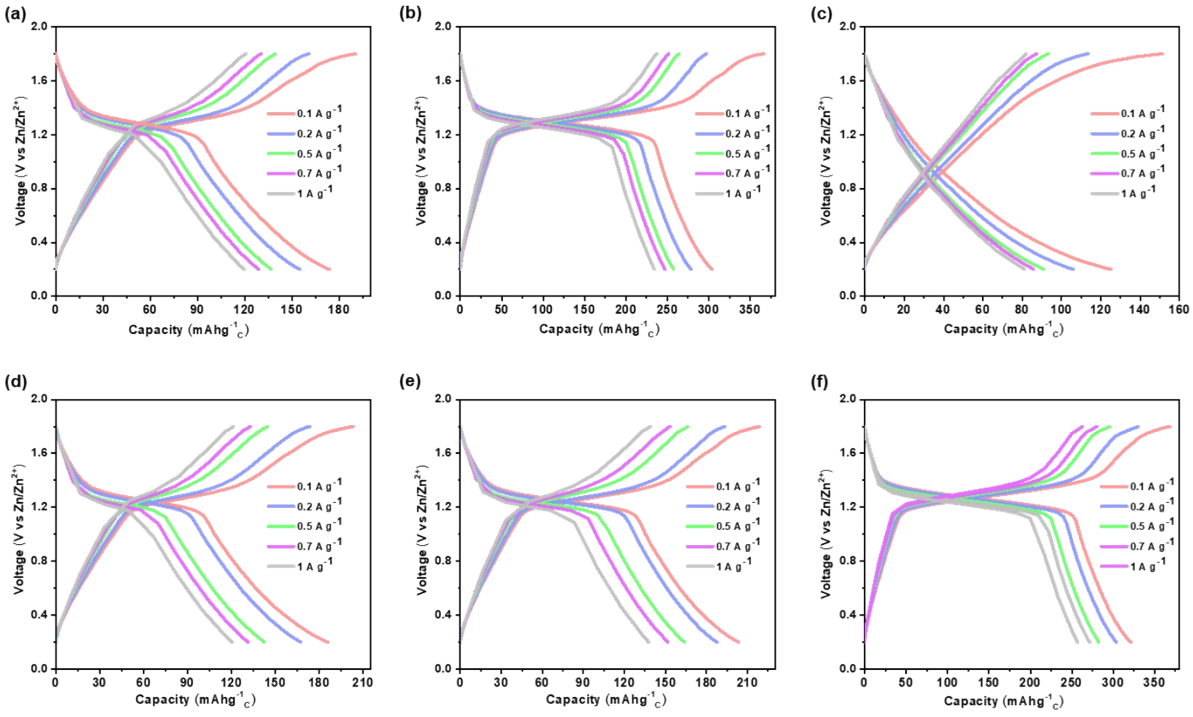

Fig. S10 GCD curves of fabricated AZHBC cells at different current densities (0.1, 0. 2, 0.5, 0.7, and 1 A g^{-1}) in (a) 1 M $ZnSO_4$ + 0.04 M KI, (b) 1 M $ZnSO_4$ + 0.16 M KI, (c) 2 M $ZnSO_4$, (d)2 M $ZnSO_4$ + 0.04 M KI, (e) 2 M $ZnSO_4$ + 0.08 M KI, and (f) 2 M $ZnSO_4$ + 0.16 M KI electrolyte solutions, respectively.

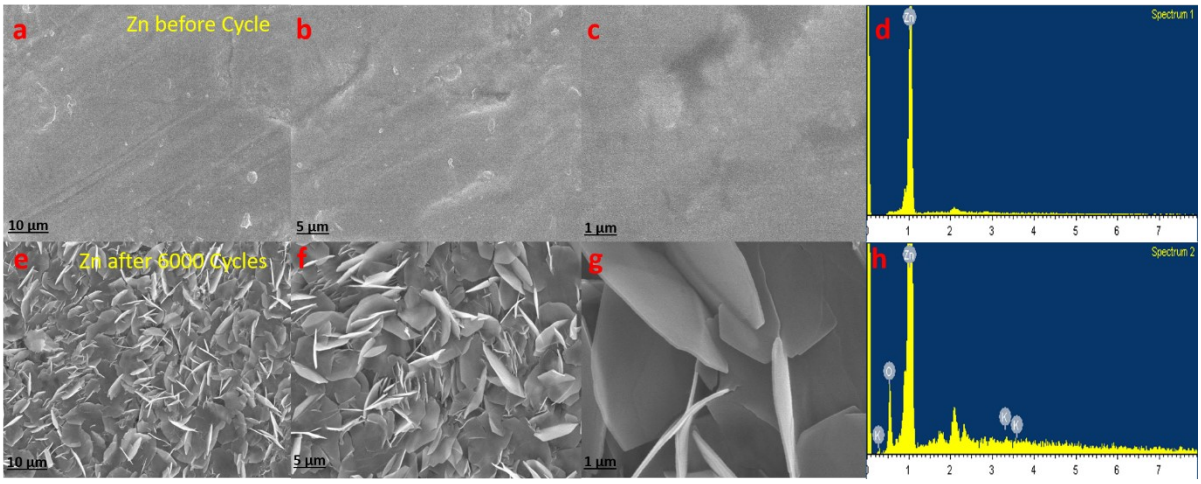

Fig. S11 SEM images and EDAX of Zinc anode (a, b, c & d) before cycle and (e, f, g & h) after 6000 cycles in 1 M $ZnSO_4$ + 0.08 M KI.

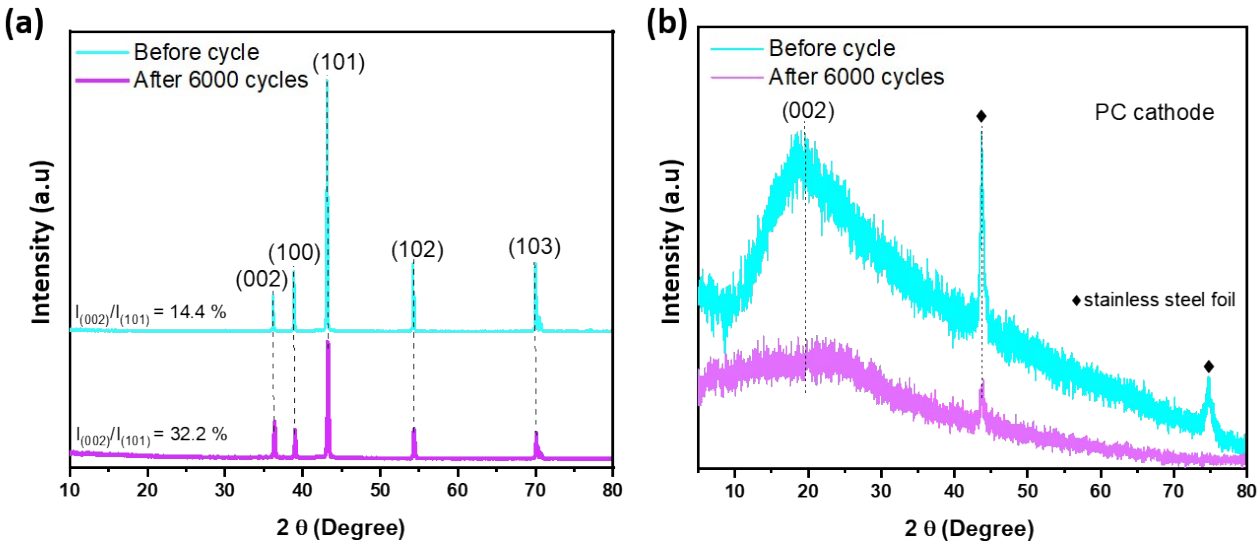

Fig. S12 XRD of (a) Zinc anodes, (b) PC cathodes before and after cycling.

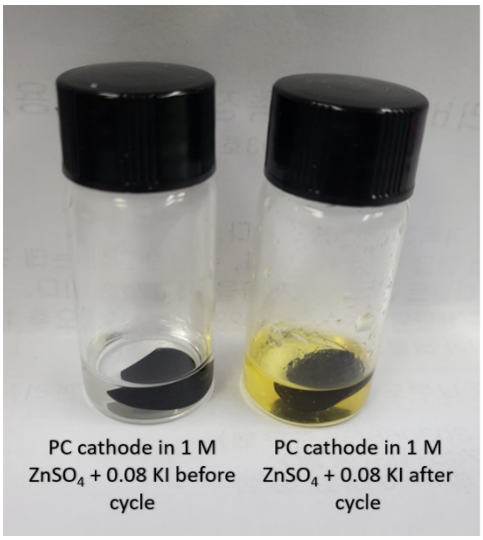

Fig. S13 Color change of electrodes immersed in fresh KI electrolyte (a) before and (b) after complete charging to confirm the presence of I_3^-.

Fig. S14 SEM images of PC cathode (a) before and (b) after 6000 cycles in 1 M $ZnSO_4$ + 0.08 M KI.

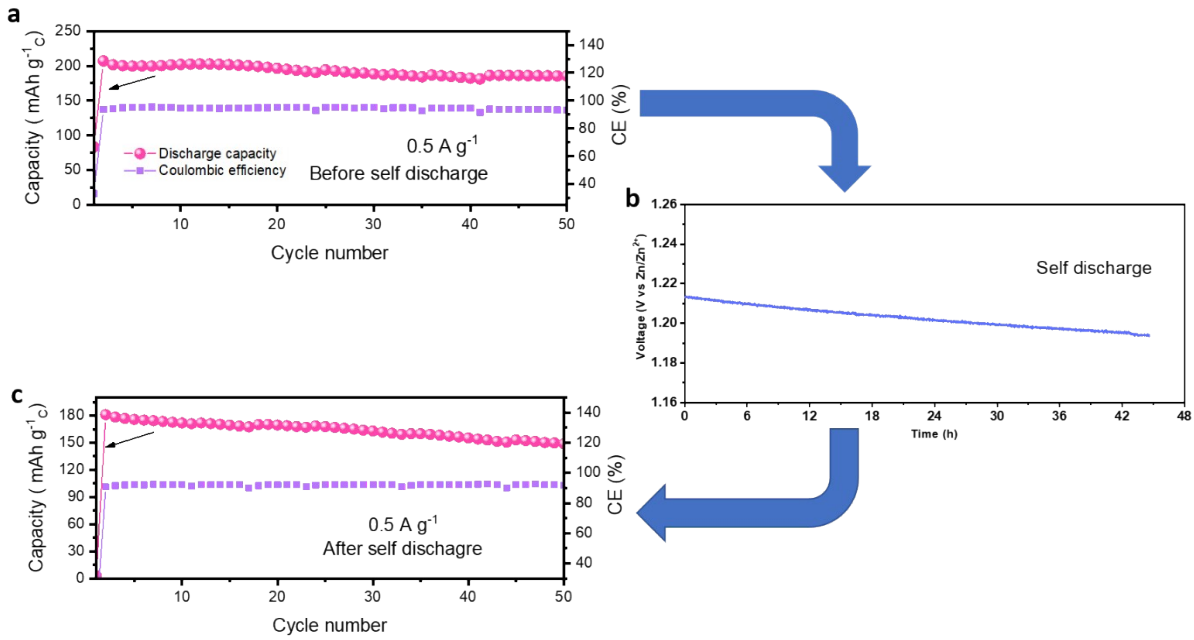

Fig. S15 (a) Cyclic stability before self-discharge (b) self-discharge and (c) Cyclic stability after self-discharge of AZHBC in 1M $ZnSO_4$ + 0.08 M KI at 0.5 A g^{-1}.

Table S2 Price comparison table of KI and ZnI_2.

Chemical/ Brand	Sigma Aldrich	Alfa Aesar
KI	**USD.** 79.14 (100 g)	**USD.** 45.76 (50 g)
ZnI_2	**USD.** 231.56 (100 g)	**USD.** 84.01 (50 g)

Cathode	**Electrolyte**	**Current Density (A g^{-1})**	**Specific Capacity (mAh g^{-1}_C)**	**Energy density (Wh kg^{-1})**	**Ref**
PCN	Aq. 1 M $ZnSO_4$	0.2	149	119	1
HPC	Aq. 1 M $ZnSO_4$ + 1M Na_2SO_4	0.2	204	118	2
PSC-A600	1 M $Zn(CF_3SO_3)_2$ in AN	0.2	183.7	147	3
O-rich PC (PC700)	Aq. 3 M $Zn(ClO_4)_2$	0.1	179.8	104.8	4
OPC	Aq Gel. 1 M $ZnSO_4$	0.2	137.7	82.36	5
MDC	Aq. 1 M $ZnSO_4$	0.2	-	36.4	6
Ca-900	Aq. 1 M $ZnSO_4$	0.1	~90	75.22	7
AC	Aq. 2 M ZnSO4	0.1	121	84	8
GH	Aq. 2 M $ZnSO_4$	0.2	99.3	76.2	9
AC	SA-Zn hydrogel	0.2	260.5	286.6	10
Kelp-carbon	2 M $Zn(CF_3SO_3)_2$ in AN	0.1	196.7	111.5	11
PC	**Aq. 2 M $ZnSO_4$ +0.16 KI**	**0.1**	**305.9**	**367.1**	**This work**
PC	**Aq. 1 M $ZnSO_4$ +0.08 KI**	**0.1**	**399.3**	**479.1**	**This work**

Table S3 Comparative electrochemical results of the fabricated KI redox active AZHBC with previously reported works on different zinc-based energy storage systems.

Table S4 EDAX results of Zinc anodes before and after 6000 cycles

(a)

Element	Weight%	Atomic%
Zn K	100.00	100.00
Totals	100.00	

(b)

Element	Weight%	Atomic%
O K	6.23	21.29
K K	0.44	0.61
Zn K	93.34	78.10
Totals	100.00	

References

1. Y. G. Lee, G. H An, *ACS Appl. Mater. Interfaces*, 2020, **12**, 41342-41349.
2. P. Yu, Y. Zeng, Y. Zeng, H. Dong, H. Hu, Y. Liu, Y Liang, *Electrochim. Acta*, 2019, **327**, 134999.
3. Z. Li, D. Chen, Y. An, C. Chen, L. Wu, Z. Chen, X. Zhang, *Energy Stor. Mater*, 2020, **28**, 307-314.
4. J. Yin, W. Zhang, W. Wang, N. A. Alhebshi, N. Salah, H. N. Alshareef, *Adv. Energy Mater.*, 2020, **10**, 2001705.
5. Y. Zheng, W. Zhao, D. Jia, Y. Liu, L. Cui, D. Wei, R. Zheng and J. Liu, Chem. Eng. J., 2020, **387**, 124161.
6. T. Xiong, Y. Shen, W. S. V. Lee, J. Xue, *Nano Materials Science*, 2020, **2**, 159-163.
7. Y. Zhang, Z. Wang, D. Li, Q. Sun, K. Lai, K. Li, L. Ci, *J. Mater. Chem. A*, 2020, **8**, 22874-22885.
8. L. Dong, X. Ma, Y. Li, L. Zhao, W. Liu, J. Cheng, F. Kang, *Energy Stor. Mater*, 2018, **13**, 96-102.
9. Y. Zhu, X. Ye, H. Jiang, J. Xia, Z. Yue, L. Wang, X. Yao, *J. Power Sources*, 2020, **453**, 227851.
10. L. Han, H. Huang, X. Fu, J. Li, Z. Yang, X. Liu, M. Xu, *Chem. Eng. J.,* 2020, **392**, 123733.
11. J. Zeng, L. Dong, L. Sun, W. Wang, Y. Zhou, L. Wei, X. Guo, *Nano-Micro Lett*, 2021,

13, 1-14.